

ORIGINAL RESEARCH ARTICLE

Synthesis and characterization of polyurethane and its nanocomposite adhesive derived from biobased isocyanate and polyol

Swarnalata Sahoo^{1,2*}, Smita Mohanty^{1,2}, Sanjay Kumar Nayak^{1,2}

¹ Laboratory for Advanced research in polymeric materials (LARPM), CIPET, Bhubaneswar 751024, India. E-mail: sahuo.swarnalata@gmail.com

² Central institute of Plastic Engineering and Technology, Chennai 600032, India

ABSTRACT

In the current research, the vegetable oil based polyurethane nanocomposite (PUNC) adhesive was prepared using transesterified castor oil (CO) based polyol, partially biobased aliphatic isocyanate (PBAI) and organically modified montmorillonite nanoclay (Closite 30B). The transesterified CO was synthesized by reacting CO with ethylene glycol, which was confirmed using proton nuclear magnetic resonance (¹HNMR) analysis. Further, the prepared polyurethane (PU) and its nanocomposite adhesive with specific NCO: OH molar ratio 1.3:1 was confirmed by Fourier transform infrared spectroscopy (FTIR) analysis. The increasing of wt% of nanoclay loading level up to 3% into PU matrix increased the lap shear strength of the adhesive systems. Subsequently, the effect of polyurethane nanocomposite adhesives on the bonding strength of wood-to-wood and aluminum-to-aluminum substrate was studied using lap shear strength test. The nanoclay was observed to effectively intercalate into the polymer matrix. Moreover, the phase separation in PU and PUNC adhesive was studied using atomic force microscope (AFM) and differential scanning calorimetry (DSC) analysis.

Keywords: Castor Oil; Biobased Isocyanate; Nanoclay; AFM

ARTICLE INFO

Received: 17 April 2021
Accepted: 10 June 2021
Available online: 15 June 2021

COPYRIGHT

Copyright © 2021 Swarnalata Sahoo *et al.*
EnPress Publisher LLC. This work is licensed under the Creative Commons Attribution-NonCommercial 4.0 International License (CC BY-NC 4.0).
<https://creativecommons.org/licenses/by-nc/4.0/>

1. Introduction

Polyurethane adhesive synthesis from renewable sources has been one of the major efforts recently being practised worldwide as an alternative to the petrochemical feedstock^[1-7]. The vegetable oils such as castor oil, soybean oil^[6], palm oil^[7], sunflower oil, corn oil and linseed oil^[8-10] have been used for the fabrication of polyurethane adhesive due to its cost effectiveness, low toxicity and health concern. Among these, castor oil (CO) offers a wide range of advantages for the formulation of polyurethane adhesive. Hence recent focus has been diverted to the castor oil based polyurethane adhesive due to the presence of a high percentage of ricinoleic acid, a monounsaturated, and 18carbon fatty acid in CO. Prior to the advantages of CO such as high reactivity, easy availability and non-toxicity, it was found to be a suitable backbone towards the development of PU adhesive. In general, castor oil contains 85–95% ricinoleic acid, 2–6% oleic acid, 1–5% linoleic acid, 0.5–1% alpha-linoleic acid, 0.5–1% stearic acid, 0.5–1% palmitic acid, 0.3–0.5% dihydroxystearic acid and 0.2–0.5% other component. The direct utilization of CO in PU adhesive gives limited hardness and structural irregularity due to the presence of secondary hydroxyl groups in CO, which exhibits low rate of curing due to the steric hindrance formation during polyurethane formation. To overcome these limitations, chemical modifications on active sides via transesterification or transamidification has been adopted to utilize the double bond of unsaturated fatty acid and carboxylic group,

to increase its hydroxyl value for improving the cross linking density and rigidity of the polyurethane network. Now a day's moisture-cured polyurethane adhesive has been synthesized from castor oil because it has many potential advantages including shear strength, flexibility and reactivity, etc., which allows polymer materials to adhere on various moist substrates through the development of strong chemical bonds^[9]. The performance of an adhesive is inter-related to its adhesion properties like viscoelastic properties, surface free energy and the adhered substrate^[10].

Generally, polyurethane consists of macrodiol which may be polyester or polyether, isocyanate, catalyst and other chain extender^[11]. Polyurethane is a two segmental structure based polymer, where a soft and hard domain produces phase separation. The phase separation is obtained due to low molecular weight of the polyol (soft domain)^[12]. The isocyanate (hard domain) is the essential part required for PU synthesis. The isocyanates containing may be two or more-NCO groups per molecule. For the formulation of polyurethane adhesive, the used isocyanates can be synthetic (aliphatic, aromatic or cycloaliphatic) or biobased in nature^[13]. To improve the limitations such as shorter gel time, low durability, deterioration in mechanical and thermal properties, methods have been analyzed with the incorporation of nanoclay within the PU matrix. Thus, the development of polyurethane adhesive with the incorporation of nanoclay has gained strong demand as these fillers are able to enhance physiochemical properties such as high adhesion strength as well as thermal stability of polyurethane nanocomposite adhesive^[14]. However, very few literatures have been explained about the synthesis and utilization of polyurethane clay nanocomposite in adhesive technology^[15-17].

The novelty of this work is the development of newly polyurethane-clay nanocomposite adhesive derived from the combination of biobased isocyanate and vegetable oil based polyol with the incorporation nanoclay (Closite 30B), which can be utilized as wood-wood bonding adhesive. However, several literatures have been reported for the development of petrobased polyurethane-clay nanocomposite adhesive^[16,17].

Hence, in the current research work, the present

investigation focused on the development of biobased polyurethane nanocomposite adhesive with the incorporation of nanoclay into the PU matrix. The authors have initiated to synthesize biobased polyurethane using biobased polyol and partially biobased aliphatic isocyanate. To observe the improved adhesion strength of PU adhesive on wood and aluminum substrate and their utilization in adhesive technology, lap shear test has been carried out. The phase separation structure in PU matrix has been studied in AFM analysis. Further, the phase separation in polyurethane adhesive was confirmed by DSC analysis.

2. Experimental procedure

2.1 Materials and methods

Ethylene glycol and castor oil were procured from M/s SD Fine chemicals, Kolkata. Partially biobased hexamethylene diisocyanate (Tolonate TM X FLO 100) was supplied by M/s Vencorex chemical, France. Dibutyl tin dialurate (DBTDL) was procured from M/s Sigma Aldrich, Germany. Analytical grade acetone and tetrahydrofuran (THF) were procured from M/s Fischer Scientific, USA. Closite 30B was supplied by Southern Clay Products, USA.

2.2 Polyurethane and its nanocomposite adhesive synthesis

The polyester polyol based polyurethane nanocomposite adhesive was prepared by two step method. In the first step, polyurethane adhesive was synthesized from modified castor oil with the addition of partially biobased aliphatic isocyanate. The castor oil was modified to obtain the polyester polyol using castor oil and ethylene glycol (EG) in the presence of lead oxide catalyst. The transesterification process of CO was performed to modify the CO under the nitrogen atmosphere to avoid oxidation reaction produced at the time of reaction. This process was carried out in a three necked round bottom flask of 250ml equipped with a magnetic stirrer, thermometer and reflux condenser with continuous stirring for 3 hr at 230 °C. The acid value of transesterified polyol was measured periodically using acetic anhydride method as described earlier^[1]. Further, the synthesized polyol was dried under vacuum at 70 °C^[12]. In the second step, the polyurethane nanocomposite

adhesive was prepared with the incorporation of nanoclay. Initially, the organically modified clay was dried for 5hr and the clay was separately mixed in THF solution with constant stirring. Then the clay was sonicated for 50min to minimize the agglomeration. After that, the solution was gradually added to the PU solution with continuous stirring of 15 min in the presence of N₂ gas environments. Then the formulated mixture was poured into the glass plate. The complete reaction mechanism is shown in **Figure 1**.

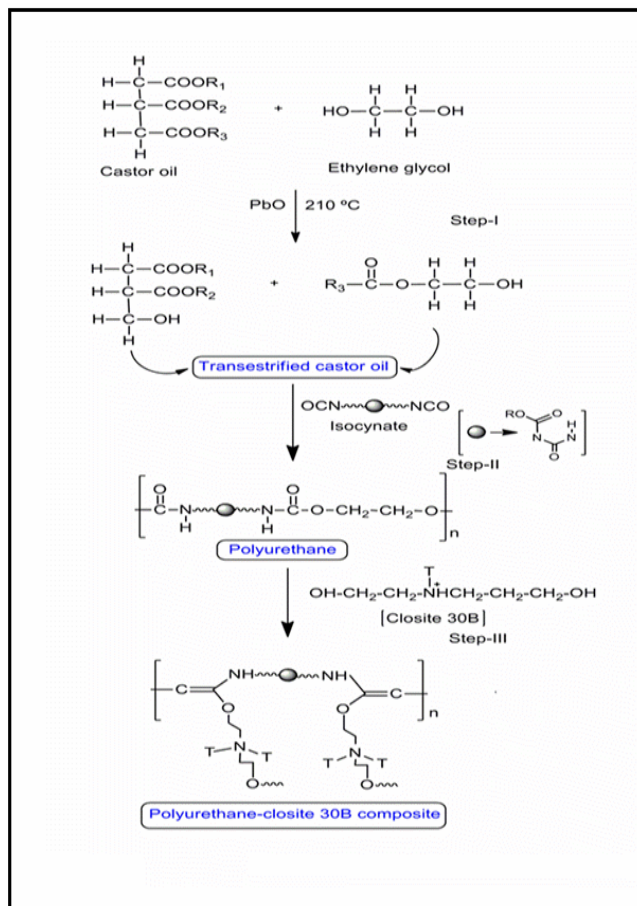


Figure 1. Synthesis mechanism of PU and PUNC adhesive.

3. Characterization

3.1 Proton nuclear magnetic resonance (¹HNMR) study

The ¹HNMR spectra of CO and transesterified castor oil based polyol were recorded by using JEOL DELTA2 500 MHz FX-1000 spectrometers (INSTROM). All measurements of chemical shift value were made using deuterated CDCl₃ solvent.

3.2 Fourier-transform infrared (FTIR) analysis

The spectra of polyurethane (PU) and

polyurethane clay nanocomposite adhesive (PUNC) samples were analyzed by FTIR (Nicolet 6700, Thermo Scientific, USA) spectra. The FTIR analysis was carried out on each sample with 64 scans with the wavelength range of 400–4000 to cm⁻¹.

3.3 Lap shear test

The required specimen for lap shear test was prepared according to the standard ASTM D 906. The substrates were dried and polished with sandpaper of grit no. 60. The prepared adhesive solution (thickness 0.1mm) was applied on both pieces of the wood and aluminum substrates by using a brush on 25x30 mm² area of overlap. Over the contact area of wood pieces, a load having 2–3 kg has been applied and left overnight. After that, the specimen joints were kept at room temperature for 10 days. Then joint substrates were tested for measuring bonding strength by lap shear strength^[18]. The shear strength bonded substrate joints were tested using a universal testing machine as per the standard ASTM D 906-82.

3.4 Wide angle X-ray diffraction (WAXD) analysis

Wide angle X-ray diffraction (WAXD) analysis was used to analyze the interlayer gallery spacing of nanoclays in the nanocomposites, using Philips X'Pert MPD (Japan), with graphite monochromator and a Cu K α radiation source operated at 40 kv and 30 mA.

3.5 Atomic force microscope (AFM) analysis

Surface morphology and phase separation of PU and PUNC adhesive sample were recorded by using AFM (M/s. Park scientific instrument, XE-100, USA) in contact mode and a commercial probe was used at room temperature and moderate pressure.

3.6 Differential scanning calorimetry (DSC) analysis

The phase separation in PU and PUNC adhesive surface and the change in *T_g* values were evaluated using (DSC) Q20, M/s, TA Instrument, USA) at a temperature range of -100 °C to 100 °C at a heating 10 °C/min under N₂ atmosphere and a flow rate of 50 mL/min.

4. Result and discussions

4.1 Proton nuclear magnetic resonance (¹HNMR) study

¹HNMR spectra of castor oil (CO) and modified CO are represented in **Figure 2** which was described in our earlier research paper^[1]. It is observed that the chemical shift δ values corresponding to 0.9 ppm and 2.3 ppm, is primarily due to methyl protons and the fatty acid proportion, respectively. Along with the above peak, the peak value δ at 4.0 attributed due to methylene protons of glycerol. The above peaks are always assumed as the reference because throughout the whole reaction the intensity of the above peak does not change. It is also observed that in CO and modified CO, the chemical shift δ values corresponding to 2.1-1.9, 1.5-1.75, 1.2-1.4 ppm, are mainly due to $-\text{CH}_2-\text{CH}=\text{}$, $\text{CH}_2-\text{CH}_2-\text{O}$ and aliphatic backbone respectively. The peaks at 3.6 and 4.1 ppm correspond to $-\text{CH}_2$ adjacent to secondary C, and $\text{CH}_2-\text{O}-\text{C}=\text{O}-$, respectively. The modification of CO is confirmed by the presence of chemical shift at δ values 3.7 and 3.8 ppm, which correspond to $-\text{CH}_2\text{OH}$ and $-\text{CHOH}$. Hence the modified polyol is confirmed through ¹HNMR.

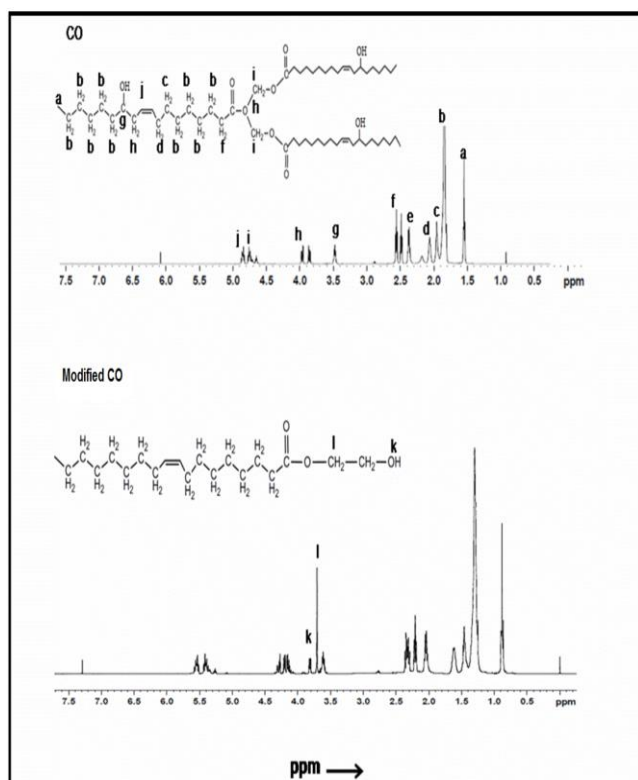


Figure 2. ¹HNMR spectra of CO and modified CO.

4.2 Fourier-transform infrared (FTIR)

analysis

The IR spectra of PU and PUNC adhesive containing 3 wt% nanoclay were recorded in **Figure 3**. As evidenced from **Figure 3**, the characteristic absorption peaks were observed at 1050 cm^{-1} due to Si-O stretching vibration. However, marginal shifting of the peaks in PU was observed in presence of Closite 30B nanoclay due to strong intermolecular H-bonding between the hydroxyl group of C 30B and hard segment ($-\text{NH}-$) of polyurethane matrix^[21]. The absorption peaks were observed at 3334 cm^{-1} due to the presence of urethane stretching. The absence of isocyanate peak at 2260 cm^{-1} indicated the completion of reaction between soft segment (OH group) and hard segment (NCO group) in both PU and PUNC adhesive. The band observed at $2923\text{--}2839\text{ cm}^{-1}$, 1735 cm^{-1} and at 1237 cm^{-1} attributed due to $-\text{CH}_2$ stretching frequencies, carbonyl urethane stretching and coupled C-N and C-O stretching respectively. Hence, the above analysis showed similar IR spectra in PU and PUNC adhesive. No such differences in position of band assignments were observed in PU and PUNC adhesive, except only change in band intensity. This fact was obtained in accordance with the preparation of PUNC adhesive by other groups. But the band position of distinct functional group of the PU was identical to those of PUNC. This fact has also been reported by other researcher, which confirmed that the presence of silicate layers does not change the chemical structure of polyurethane^[19]. To assure the chemical interaction between nanoclay and the individual components of polyurethane, the FTIR study confirmed the complete reaction obtained in PUNC surface.

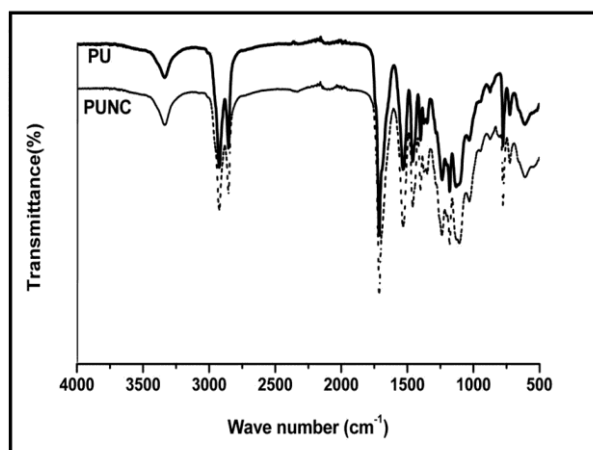


Figure 3. FTIR studies of PU and PUNC adhesive sample.

4.3 Lap shear test

The effect of PU matrix after the incorporation of 0 to 5wt % of nanoclay is depicted in **Figure 4** and the corresponding shear strength values are summarized in **Table 1**. The result showed the improvement of bonding strength with the increase in clay content. It is found that the integration of 3 wt % of nanoclay throughout the PU matrix showed higher bonding strength, which was taken as optimum composition. After that, the lap shear strengths of optimize PU and PUNC adhesive with respect to the substrates such as wood and aluminum (Al) respectively are depicted in **Table 2**. From the analytical observation, it has been found that the shear strength of PU adhesive for both the substrates increases with the increase in a span of days. The PU adhesive exhibited 40.23, 50.41, 69.20 and 69.22 ($N/m^2 \times 10^5$) lap shear strength of wood-wood substrate after the period of 10, 20, 30 and 40 days respectively. Similarly, the lap shear strength of PU adhesive with respect to Al-Al substrate bonding exhibited 32.15, 44.32, 65.01 and 65.03 ($N/m^2 \times 10^5$) after the period of 10, 20, 30 and 40 days. In the meantime, after the incorporation nanoclay throughout the PU matrix, the developed PUNC adhesive exhibited 72, 85, 103.07 and 103.09 ($N/m^2 \times 10^5$) lap shear strength of wood-wood substrate after 10, 20, 30, and 40 days respectively, and 32.15, 44.32, 65.03 and 65.04 ($N/m^2 \times 10^5$) lap shear strength of Al-Al substrate after the duration of 10 days, 20 days, 30 days and 40 days respectively. Hence it can be concluded that addition of 3wt % of clay content in PU matrix showed better adhesion strength over the neat PU. This might be due to the strong interfacial adhesion between the substrate and the adhesive. The failure process of joint bonding substrate was a cohesive failure, which confirmed the strong interfacial interaction between the adhesive and substrate^[20,21]. This trend was in accordance with the strong interfacial interaction between the OH group of OMMT clay with the OH group in Al and OH group on wood substrate respectively. Further, it is noticed that, the shear strength of PU adhesive to hold the substrates increase up to 30 days, after that the shear strength for both substrates gradually leveled off. This result also indicated that higher shear strength in wood-wood substrate as compared to Al-Al substrate is due to the presence of high

amount of polar hydroxyl group in wood substrate that produced strong interaction between wood substrate and adhesive. Hence, in the current study of view, wood substrates were chosen as the suitable substrate for PU and PUNC adhesive.

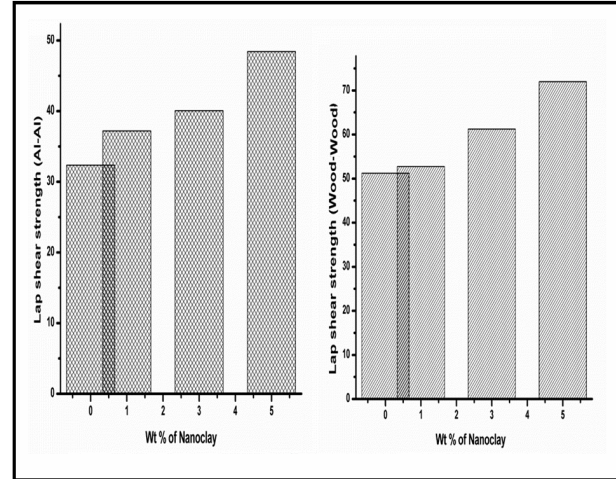


Figure 4. Lap shear strength of wood-wood bonding and Al-Al bonding substrate.

Table 1. Lap shear strength of substrates upon incorporation of different wt% of nanoclay

Sample code	Wood-Wood bonding strength of PUNC after 10 days ($N/m^2 \times 10^5$)	Al-Al bonding strength of PUNC after 10 days ($N/m^2 \times 10^5$)
0 wt% nanoclay	51.23	32.33
1 wt% nanoclay	52.75	37.21
3 wt% nanoclay	61.23	40.05
5 wt% nanoclay	72	48.44

Table 2. Comparison of lap shear strength between the substrates with PU and PUNC adhesive

No. of days	Wood-Wood		Al-Al	
	Lap shear strength ($N/m^2 \times 10^5$)	Lap shear strength ($N/m^2 \times 10^5$)	Lap shear strength ($N/m^2 \times 10^5$)	Lap shear strength ($N/m^2 \times 10^5$)
	PU	PUNC	PU	PUNC
10 days	40.23	72	32.15	48.45
20 days	50.41	85	44.32	52.16
30 days	69.20	103.07	65.03	71.23
40 days	69.22	103.09	65.04	71.23

4.4 Wide angle X-ray diffractometer (WAXD) analysis

WAXD diffraction pattern was carried out in order to investigate the dispersion of OMMT clay throughout the PU matrix as represented in **Figure 5**. A strong diffraction peak was appeared at $2\theta = 5.09^\circ$ for OMMT nanoclay. The disappearance of this peak at $2\theta = 5.09^\circ$ in PUNC adhesive film confirming the strong interaction of clay and PU matrix. This indicated the increase in distance from a certain plane in one layer corresponding to another layer of the plane. Hence the diffraction was observed and the basal of the polymer can be calculated by using brags law $d \sin \Theta = n\lambda$. The diffraction peaks of all synthesized PU and PUNC adhesive films were found to be $2\theta^\circ$ whereas the corresponding basal spacing were 4.23 and 4.43 Å respectively, thereby indicating the increase in gallery height in PUNC adhesive film from PU adhesive film by 0.20 Å. Thus the higher value of basal spacing indicates that the silicate layers in polyurethane molecular chains are intercalated without exfoliation in the system. This indicated that the galleries of clay layers expanded in the PUNC sample^[18]. In addition, the peak intensity of nanocomposite is lowered with the addition of nanoclay, which reveals that there is a homogenous dispersion of nanoclay within the PU matrix.

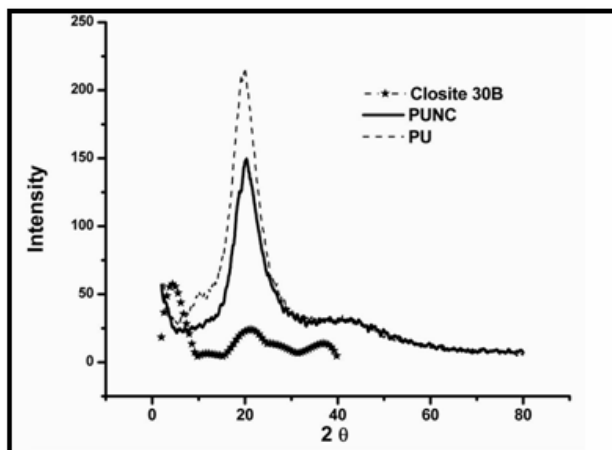


Figure 5. XRD analysis of PU and PUNC adhesive film.

4.5 Atomic force microscopy (AFM) analysis

The surface roughness at the nanometer level and phase morphology of PU and PUNC adhesive were studied using AFM non-contact mode represented in **Figure 6**. From the topographical images, it was observed that the phase separation obtained in the polyurethane due to the incompatibility of hard and soft domain. The higher degree of phase

segregation was obtained after the incorporation of nanoclay (3 wt%) into the PU matrix. This can be attributed to the good interaction, such as H-bonding, polar-polar, etc. between the clay and hard domains of polyurethane (PU) adhesive film. Moreover, the degree of phase segregation was found to be 0.9° and 0.56° of PUNC and PU adhesive film respectively. Further, the brighter region indicates the isocyanate rich dispersed hard phase and the darker region indicates the polyol rich dispersed soft phase. Whereas, after the incorporation of nanoclay, it has been revealed the diameter of the hard segments was expanded^[18]. From the topographical image in **Figure 6**, the average roughness (R_a) of PU and PUNC has been obtained to observe the structural changes in the surface. The surface roughness R_a of PU was found to be 19.42 nm whereas PUNC adhesive film exhibited 17.09 nm. The decrease in roughness and inhomogeneity in PUNC adhesive film was due to the addition of NC on PU matrix as a result of the good interaction between clay and PU^[22–24].

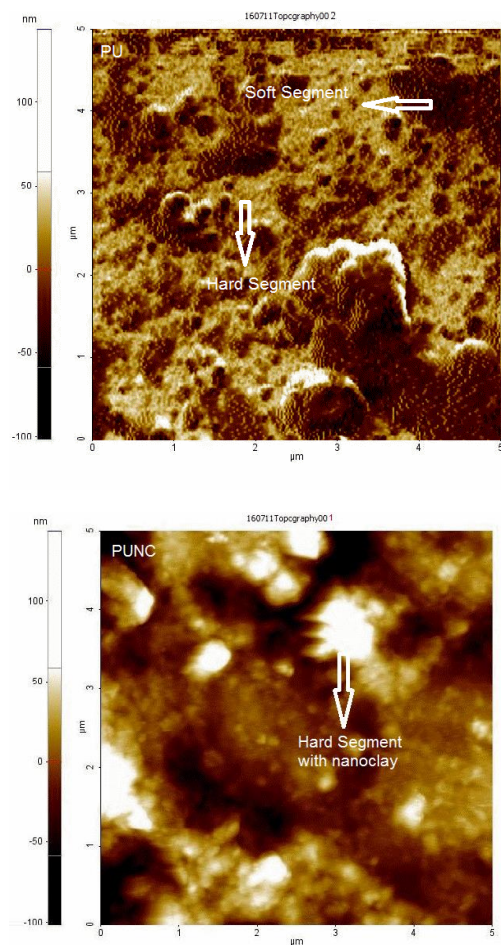


Figure 6. AFM analysis of PU and PUNC adhesive film.

4.6 Differential scanning calorimetry analysis (DSC)

Differential scanning calorimetry analysis (DSC) was performed to investigate the effect upon the addition of nanoclay into the PU adhesive reported in **Figure 7**. The analysis showed two step transitions due to the presence of two T_g values corresponding to the soft and hard segment. This indicates the occurrence of phase segregation on the structure of PU and PUNC adhesive. Hence, in phase segregation structure, the higher T_g value in PUNC restricts the polymer chain motion which induced due to higher crosslink density and an increase in free volume of the nanocomposites. The similar results have also been reported on the earlier research^[25,26]. In addition, it has been observed that the T_g of soft segment and hard segment was shifted to higher temperature upon the loading of nanoclay on the PU matrix. The T_g values of soft segment corresponding to PU and PUNC were found to be $-37.8\text{ }^\circ\text{C}$ and $-27.3\text{ }^\circ\text{C}$ respectively. In the meantime, the T_g of hard segment corresponding to PU and PUNC was found to be $70\text{ }^\circ\text{C}$ and $74.2\text{ }^\circ\text{C}$ respectively. The above result indicated that, the PUNC exhibits higher T_g and cross linking density upon the incorporation of 3 wt% of nanoclay within the PU matrix. Further, in PUNC, the marginal increase in T_g value in hard segment and soft segment indicates the good interaction between the H-H bonding of PU and nanoclay.

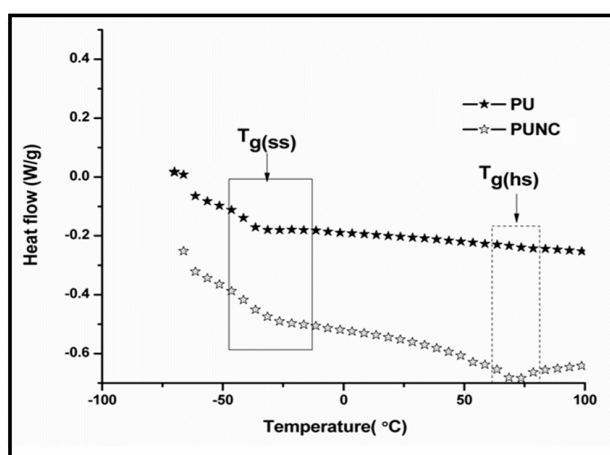


Figure 7. DSC analysis of PU and PUNC adhesive.

5. Conclusions

In the present work, a simple approach for the development of vegetable oil based PU and PUNC

adhesive with the incorporation of nanoclay loading using in-situ polymerization method via ultrasonication technique have been reported. The developed adhesives were confirmed using FTIR analysis. The adhesive samples containing 3 wt% of nanoclay showed higher adhesion shear strength over the PU adhesive. Further, the adhesion strength of adhesive with respect to the wood substrate showed higher shear strength compared to Aluminum (Al) substrate. The dispersive characteristics of nanoclay into the PU matrix were confirmed by WAXD analysis and subsequently the formation of the phase separation structure was verified by AFM analysis. The analysis resulted that the nanoclay layers were well dispersed and the phase separation was prominently appeared on the surface of polyurethane. Further confirmation of phase separation was studied using DSC analysis. In the meanwhile, the shifting of peak temperature towards higher temperature was observed upon the incorporation of nanoclay within the PU matrix. From the above discussions, it can be concluded that the bio-based PUNC adhesive synthesized from bio raw materials can be suitably used as a bioadhesive.

Conflict of interest

The authors declare that they have no conflict of interest.

References

1. Sahoo S, Kalita H, Mohanty S, *et al.* Synthesis of vegetable oil-based polyurethane: A study on curing kinetics behavior. *International Journal Chemical Kinetics* 2016; 48(10): 622–634.
2. Modesti M, Lorenzetti A, Simioni F, *et al.* Expandable graphite as an intumescent flame retardant in polyisocyanurate–polyurethane foams. *Polymer Degradation and Stability* 2002; 77(2): 195–202.
3. Weiss KD. Paint and coatings: A mature industry in transition. *Progress in Polymer Science* 1997; 22(2): 203–245.
4. Liu L, Qi Z, Zhu X. Studies on nylon 6/clay nanocomposites by melt-intercalation process. *Journal of Applied Polymer Science* 1999; 71: 1133–1138.
5. Campanella L, Bonnaillie M, Wool RP. Polyurethane foams from soyoil-based polyols. *Journal of Applied Polymer Science* 2009; 112(4): 2567–2578.
6. Miao S, Sun L, Wang P, *et al.* Soybean oil-based polyurethane networks as candidate biomaterials: Synthesis and biocompatibility. *European Journal of Lipid Science and Technology (Special Issue: European Fed Lipid Highlights)* 2012; 114(10): 1165–1174.

7. Kong XH, Yue J, Narine SS. Fatty acid-derived diisocyanate and biobased polyurethane produced from vegetable oil: Synthesis, polymerization, and characterization. *Biomacromolecules* 2009; 10(4): 884–891.
8. Chian KS, Gan LH. Development of a rigid polyurethane foam from palm oil. *Journal of Applied Polymer Science* 1998; 68(3): 509–515.
9. Tanaka R, Hirose S, Hatakeyama H, *et al.* Preparation and characterization of polyurethane foams using a palm oil-based polyol. *Bioresource Technology* 2008; 99(9): 3810–3816.
10. Somani KP, Kansara SS, Patel NK, *et al.* Castor oil based polyurethane adhesives for wood-to-wood bonding. *International Journal of Adhesion and Adhesives* 2003; 23(4): 269–275.
11. Berezkin Y, Urick M. Modern polyurethanes: overview of structure property relationship. *ACS Symposium Series* 2013; 1148: 65–81.
12. Pratheep KA, Raghunatha RK, Sravendra R, *et al.* Synthesis, characterization, and performance evaluation of novel stabilized TDI-based polyurethane coatings under accelerated weathering. *Journal of Vinyl & Additive Technology* 2005; 11(1): 13–20.
13. El-Fattaha MA, El Saeed AM, Dardira MM, *et al.* Studying the effect of organo-modified nanoclay loading on the thermal stability, flame retardant, anti-corrosive and mechanical properties of polyurethane nanocomposite for surface coating. *Progress in Organic Coatings* 2015; 89: 212–219.
14. Hu Y, Song L, Xu J. Synthesis of polyurethane/clay intercalated nanocomposites. *Colloid and Polymer Science* 2001; 279: 819–822.
15. Nik Pauzi NNP, Majid RA, Dzulkifli MH, *et al.* Development of rigid bio-based polyurethane foam reinforced with nanoclay. *Composites Part B: Engineering*, 2014; 67: 521–526.
16. Zeng Q, Yu A, Lu G. Interfacial interactions and structure of polyurethane intercalated nanocomposite. *Nanotechnology* 2005; 16(12): 2757–2763.
17. Swain S, Sharma RA, Bhattacharya S, *et al.* Pegular papers: Effects of nano-silica/nano-alumina on mechanical and physical properties of polyurethane composites and coatings. *Transactions on Electrical and Electronic Materials* 2013; 14(1): 1–8.
18. Verma G, Kaushik A, Ghosh AK. Nano-interfaces between clay platelets and polyurethane hard segments in spray coated automotive nanocomposites. *Progress in Organic Coatings* 2016; 99: 282–294.
19. Patel S, Bandyopadhyay A, Ganguly A, *et al.* Synthesis and properties of nanocomposite adhesives. *Journal of Adhesion Science and Technology* 2006; 20(4): 371–385.
20. Chethana M, Madhukar BS, Siddaramaiah SR. Structure–property relationship of biobased polyurethanes obtained from mixture of naturally occurring vegetable oils. *Advances in Polymer Technology* 2014; 33(1): 21390.
21. Kong X, Narine SS. Physical properties of polyurethane plastic sheets produced from polyols from canola oil. *Biomacromolecules* 2007; 8(7): 2203–2209.
22. Lan Q, Haugstad G. Characterization of polymer morphology in polyurethane foams using atomic force microscopy. *Journal of Applied Polymer Science* 2011; 121(5): 2644–2651.
23. Dekaa H, Karak N. Bio-based hyperbranched polyurethane/clay nanocomposites: adhesive, mechanical, and thermal properties. *Polymers for Advanced Technologies* 2011; 22(6): 973–980.
24. Maiti M, Bhowmick AK. New insights into rubber-clay nanocomposites by AFM imaging. *Polymer* 2006; 47(17): 6156–6166.
25. Pedrazzoli D, Manas-Zloczower I. Understanding phase separation and morphology in thermoplastic polyurethanes nanocomposites. *Polymer* 2016; 90: 256–263.
26. Wang L, He X, Wilkie CA. The utility of nanocomposites in fire retardancy. *Materials* 2010; 3(9): 4580–4606.